

UDC 528.8.04

INVESTIGATING THE IMPACT OF PAN SHARPENING ON THE ACCURACY OF LAND COVER MAPPING IN LANDSAT OLI IMAGERY

Komeil ROKNI^{ORCID}**Department of Geomatic Engineering, Faculty of Engineering, Gonbad Kavous University, Golestan, Iran*

Received 17 July 2021; accepted 17 February 2023

Abstract. Pan Sharpening is normally applied to sharpen a multispectral image with low resolution by using a panchromatic image with a higher resolution, to generate a high resolution multispectral image. The present study aims at assessing the power of Pan Sharpening on improvement of the accuracy of image classification and land cover mapping in Landsat 8 OLI imagery. In this respect, different Pan Sharpening algorithms including Brovey, Gram-Schmidt, NNDiffuse, and Principal Components were applied to merge the Landsat OLI panchromatic band (15 m) with the Landsat OLI multispectral: visible and infrared bands (30 m), to generate a new multispectral image with a higher spatial resolution (15 m). Subsequently, the support vector machine approach was utilized to classify the original Landsat and resulting Pan Sharpened images to generate land cover maps of the study area. The outcomes were then compared through the generation of confusion matrix and calculation of kappa coefficient and overall accuracy. The results indicated superiority of NNDiffuse algorithm in Pan Sharpening and improvement of classification accuracy in Landsat OLI imagery, with an overall accuracy and kappa coefficient of about 98.66% and 0.98, respectively. Furthermore, the result showed that the Gram-Schmidt and Principal Components algorithms also slightly improved the accuracy of image classification compared to original Landsat image. The study concluded that image Pan Sharpening is useful to improve the accuracy of image classification in Landsat OLI imagery, depending on the Pan Sharpening algorithm used for this purpose.

Keywords: Landsat 8 OLI, image classification, support vector machine, land cover mapping, Pan Sharpening.

Introduction

Satellite image derived land cover maps are the primary sources used in various applications, such as site selection (Eskandari et al., 2015), food security and agricultural management (Oetter et al., 2001; Pérez-Hoyos et al., 2017), flood monitoring (Zope et al., 2017), landslide susceptibility (Meneses et al., 2019), and global warming (Lawrence & Chase, 2010), hence efforts to improve the accuracy of obtained land cover maps from satellite images is very important. A huge number of studies on land cover mapping using remote sensing data has been published during the last two decades, in which different methods to generate land cover maps were utilized by the researchers (Inglada et al., 2017; Li et al., 2018; Pflugmacher et al., 2019; Ghorbanian et al., 2020; Dong et al., 2021). By reviewing the past studies it was found that different classification methods have been utilized for mapping land cover/use, such as unsupervised (ISODATA and K-means (Vijayalakshmi et al., 2021)), supervised (e.g. Mahalanobis distance, maximum likelihood, support vector machine, and artificial

neural network (Ghayour et al., 2021)), subpixel-based (Sood et al., 2021), and object-based (Shakya et al., 2021) classification techniques.

Pan Sharpening, also known as image fusion, is the process of pixel-based integration of different images of a scene, to create a new single and merged image that contains more information comparing any of the original data (Pohl & Van Genderen, 1998). Normally, Pan Sharpening techniques are used to sharpen a multispectral image with low resolution by using a panchromatic image with higher resolution, to generate a multispectral image with high resolution (Rokni et al., 2011). Various Pan Sharpening techniques have been developed, such as Intensity-Hue-Saturation (Carper et al., 1990), Brovey (Gillespie et al., 1987), Wavelet Transform (Yocky, 1995), Smoothing Filter (Liu, 2000), Pansharpen (Zhang, 2002), Principal Components Analysis (Chavez et al., 1991), High Pass Filter (Schowengerdt, 1980), and statistical-based Local Mean Matching (De Béthune et al., 1998). The benefits of image fusion have been demonstrated in many fields, such as forest (Walker et al., 2012), land use/land cover

*Corresponding author. E-mail: rokni@gonbad.ac.ir

(Santos & Messina, 2008), agricultural (Meng et al., 2011), and flood monitoring (Qiu & Qiu, 2011). Image fusion have the advantages of improving spatial resolution and interpretability of images (Pohl & Van Genderen, 1998), enhancing the aesthetic and cosmetic qualities (Carper et al., 1990), providing the ability of stereo-viewing for stereo-photogrammetry (Bloom et al., 1988), improving classification accuracy (Solberg et al., 1994), enhancing the certain features which are not visible in either of single images alone (Leckie, 1990), substituting missed information (Aschbacher & Lichtenegger, 1990), replacing defective data (Suits et al., 1988), and change detection (Du et al., 2013).

The present study aims at assessing the impact of Pan Sharpening on the accuracy of image classification and land cover mapping in Landsat 8 OLI imagery. The reason to select Landsat-8 OLI imagery for this purpose is that the Landsat-8 OLI is one of the latest and most popular satellite images which was used in recent remote sensing studies, especially for land cover mapping. It may be due to its free accessibility, various spectral bands appropriate for various applications, good spatial resolution, as well as global coverage. On the other hand, producing land cover maps, as the primary source in many scientific disciplines, is one of the most common uses of satellite imagery. In this respect, different Pan Sharpening methods were executed to merge the panchromatic band (15 m) with the visible and infrared bands (30 m) of Landsat-8 OLI imagery to generate a new multispectral image with a higher spatial resolution (15 m). Subsequently, the support vector machine (SVM), as one of the highest accuracy image classification techniques, was applied to classify the original Landsat and resulting Pan Sharpened images to generate the map of land cover types available in the study area. The results were then compared through the generation of confusion matrix and calculation of kappa coefficient and overall accuracy to assess how much Pan Sharpening can improve the accuracy of image classification in Landsat OLI imagery.

1. Material and methods

1.1. Dataset and test site

Since this study aims at assessing how much Pan Sharpening can improve the accuracy of image classification using

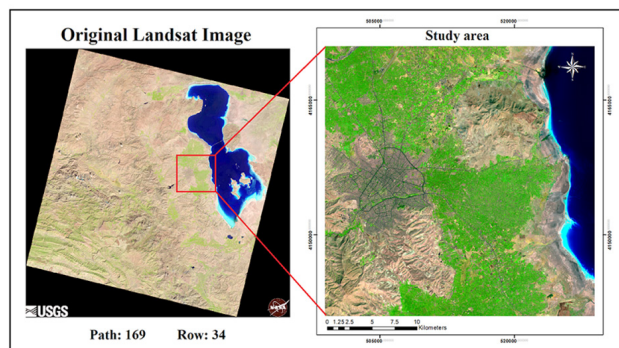


Figure 1. The original Landsat data of study area

Landsat-8 Operational Land Imager (OLI) imagery, one scene of Landsat-8 OLI surface reflectance level-2 product acquired in October 2019 were achieved from the USGS EarthExplorer. The acquired data was atmospherically corrected and pre-georeferenced. The test site in this study is the city of Urmia and the surrounding areas (Northwest of Iran). The important land cover types available in the test site are including urban and built-up area, vegetation cover, bare land, and water body. Figure 1 displays the test site in the obtained Landsat data. Table 1 present the specifications of Landsat image used in this study.

Table 1. The specifications of Landsat-8 OLI imagery

Satellite	Sensor	Path	Row	Year	Resolution (m)	Wavelength (μm)
Landsat-8	OLI	169	34	2019	30	Band 1 (0.435–0.451)
					30	Band 2 (0.452–0.512)
					30	Band 3 (0.533–0.590)
					30	Band 4 (0.636–0.673)
					30	Band 5 (0.851–0.879)
					30	Band 6 (1.566–1.651)
					30	Band 7 (2.107–2.294)
					15	Band 8 (0.503–0.676)

1.2. Pan Sharpening

To perform image Pan Sharpening, a panchromatic data with high resolution and a multispectral image with a lower spatial resolution are required. On the other hand, there are various factors to be considered before performing Pan Sharpening: the application for which the fused data is to be used, co-registration of input data, resampling method, and viewing angle of the images (Pohl & Van Genderen, 1998; Hall & Llinas, 2001). These factors are considered, since we are using the panchromatic and multispectral bands of one scene image for performing Pan Sharpening. In this study, four popular Pan Sharpening algorithms including Color Normalized (Brovey), Gram-Schmidt, NNDiffuse, and Principal Components were examined to merge the panchromatic band 8 (15 m) and multispectral bands 1–7 (30 m) of Landsat OLI imagery to achieve a multispectral image with a spatial resolution of 15 m.

Brovey (Color Normalized) transform is a simple numerical technique useful to combine data from different sensors (Amarsaikhan et al., 2012). It is named for color standardization transformation fusion and it was developed for increasing the contrast in the ends of the images histogram. This technique is not useful if conserving the radiometry of original image is essential, nevertheless it is appropriate for generating suitable images for visual

interpretation (Nikolakopoulos, 2008). This technique uses a mathematical integration of the multispectral image and panchromatic data; so that each band of the multispectral image is then multiplied using a ratio of the panchromatic image divided by sum of the multispectral bands. In this technique, only three bands are used (Karathanassi et al., 2007; Zhu, 2011).

Gram-Schmidt (GS) fusion technique usually produces a reliable result in merging images from one sensor, however the output result may vary depending on the input datasets (Klonus & Ehlers, 2009). In order to fuse the input images using this method, a process of simulating a panchromatic image from a multispectral data is implemented. It can be done by averaging the multispectral image bands. Then, a Gram-Schmidt transformation is performed to the simulated data. Subsequently, the panchromatic data is replaced with the first Gram-Schmidt band. Lastly, an inverse GS transformation is performed to create the fused output (Klonus & Ehlers, 2007; Laben et al., 2000).

NNDiffuse technique is useful when the spectral response function of multispectral image bands have least overlap with each other, also combination of all multispectral image bands cover the spectral range of the panchromatic band (Sun et al., 2014). The following are the requirements for running the NNDiffuse Pan Sharpening algorithm (Sun et al., 2014):

- The low resolution image pixel size should be an integral multiple of the high resolution image pixel size. Otherwise, resample the raster.
- The raster must be in the same projection information. Otherwise, reproject the raster.
- The raster should be aligned. Otherwise, register the raster.
- Ensure that the raster line up, especially in the upper left corner.

Principal Components (PC) transform is a rigorous statistical-based fusion approach which transforms a multivariate images of correlated variables into a new dataset of uncorrelated linear integration of the original variables. This method is suitable when we require the original image radiometry (color balance) of the input multispectral data (De Béthune et al., 1998; Klonus & Ehlers, 2009). In this algorithm:

- The first principal component is comprised of only overall luminance of data, and all inter-band variations are contained in other principal components, and
- Scene luminance is identical in the Visible and SWIR bands.

With the above assumptions, the forward transformation is performed to make to the Principal Components. Next, by removing the first principal components, its numerical range will be defined. The panchromatic band is then remapped without changing the histogram shape, but its numerical range is the same as the first PC. Subsequently, it is replaced with the PC-1, and finally the reverse transformation is applied to obtain the fused image.

In this process, it is important that the mathematics of the reverse transform does not distort the thematic information (Zhang, 2004; Helmy et al., 2010).

1.3. Image classification

Image classification was used to classify the original multispectral Landsat and the resulting Pan Sharpened images to map land cover types in the test site. In this respect, the support vector machine (SVM) approach was used to classify the images to four main land covers in the study area including: urban and built-up area, vegetation cover, bare land, and water body. The specified land cover types were visually detectable in the Landsat image, therefore the training data to perform image classification were defined through the visual inspection of the original image with help from the google earth.

SVM approach is a statistical-learning-theory based supervised classification method. This technique aims at determining the location of decision boundaries which create the best separation of the image classes (Pal & Foody, 2012; Petropoulos et al., 2012). In present work, a multi-class support vector machine pair-wise image classification was implemented. In SVM classification, selection of a suitable kernel type is an essential factor. To execute the pair-wise SVM approach in this study, the Radial-Basic-Function kernel was carried out. The reason to use this kernel was based on the fact that setting on a few parameters is needed to run it and provides reliable results (Petropoulos et al., 2012). To produce the best possible outcome, the penalty value was set in to a value of 100 in this study. In addition, the pyramid parameter was set to zero for full resolution image processing. Lastly, a probability threshold (zero) was used to make sure all the pixels of the image are classified.

1.4. Accuracy assessment

The achieved results were then compared through the generation of confusion matrix and calculation of kappa coefficient and overall accuracy to assess the impact of Pan Sharpening in improving the accuracy of land cover mapping in Landsat OLI imagery. The reference data to generate confusion matrix were defined through digitizing multiple polygons within different land cover classes in the study area using visual inspection of original Landsat image (true-color composition) with the help of google earth.

2. Results and discussion

The original Landsat image (panchromatic band 8 and multispectral bands 1–7), and the outputs of Brovey, Gram-Schmidt, NNDiffuse and Principal Components Pan Sharpening algorithms are shown in Figure 2. An investigation on the resulting fused images indicated that the outcome of Brovey algorithm is superior to other techniques for visual interpretation and detection of different land cover types in the study area.

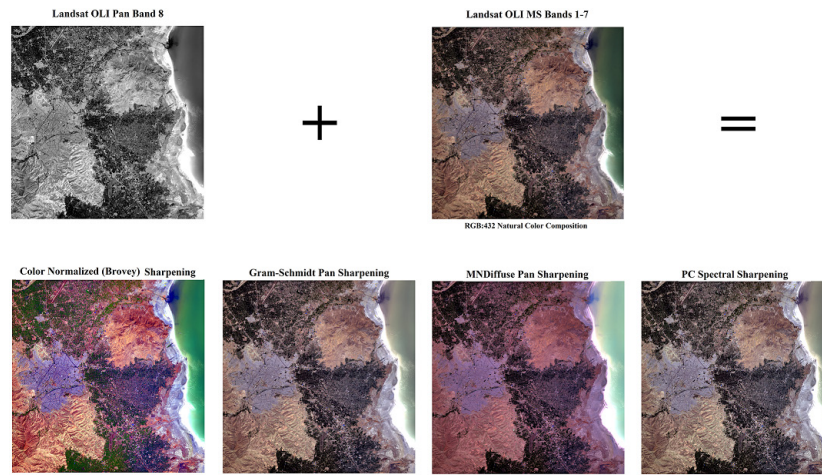


Figure 2. The original Landsat OLI and Pan Sharpened images

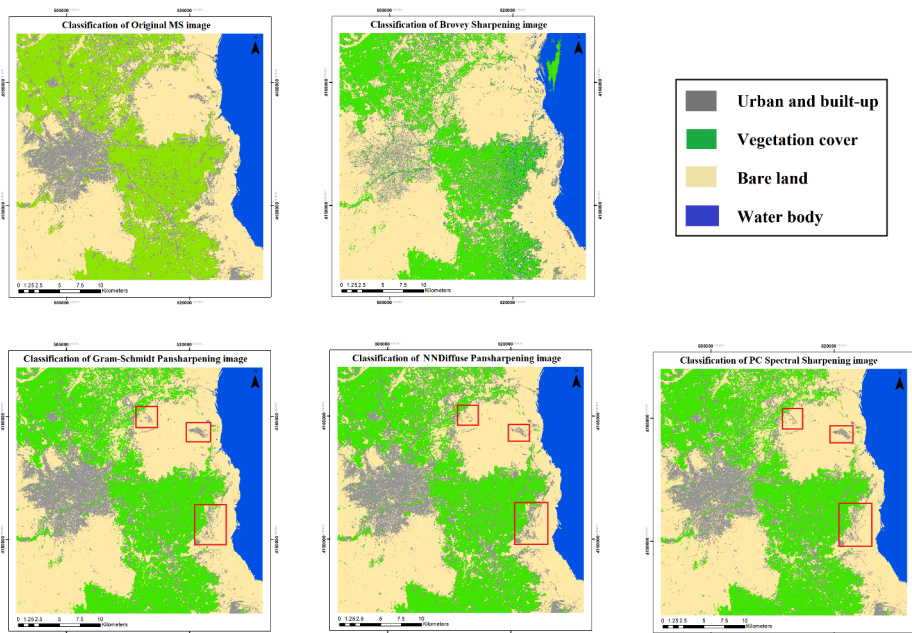


Figure 3. The generated land cover maps using the original and Pan Sharpened images

Subsequently, support vector machine approach was performed to classify the original and resulting fused images to four important land cover types available in the study region including urban and built-up area, vegetation cover, bare land, and water body. The generated land cover maps using the original and Pan Sharpened images are displayed in Figure 3. Some of the visually differences between the Gram-Schmidt, NNDiffuse and PC Spectral Sharpening classification results are highlighted. However, most differences are observed in the rate of urban density.

Visual inspection of the obtained land cover maps indicated obvious difference between the result of Brovey algorithm and other classified images. Brovey is primarily suitable for visual analysis and is not good at transforming Blue band, therefore, in classified image some errors are appeared, e.g. in water body. Nevertheless, for better evaluation and assessing the impact of Pan Sharpening on

accuracy of image classification in Landsat OLI imagery, confusion matrix were generated, consequently kappa coefficient and overall accuracy were calculated for the generated land cover maps. The accuracy assessment analysis are presented in Table 2.

Table 2. Accuracy assessment analysis

Pan Sharpening algorithm	Overall accuracy (%)	Kappa coefficient
Original image	98.21	0.972
Brovey	94.27	0.910
Gram-Schmidt	98.45	0.976
NNDiffuse	98.66	0.980
Principal Components	98.25	0.973

The results indicated that although Brovey algorithm provided reasonable output for visual interpretation, this algorithm is not appropriate for image classification. An overall accuracy and kappa coefficient of about 94.27% and 0.91 are resulted for the Brovey classified image that is specifically inferior result comparing to other classified images. On the other hand, the results revealed that the Gram-Schmidt, NNDiffuse, and Principal Components algorithms could improve the accuracy of classification and land cover mapping compared to original Landsat image. The best classification result is belonging to the NNDiffuse algorithm, which provided an overall accuracy and kappa coefficient of about 98.66% and 0.98, respectively.

The Gram-Schmidt and Principal Components algorithms also provided reliable results for this purpose. An overall accuracy of about 98.45% and 98.25% and kappa coefficient of about 0.976 and 0.973 are achieved for the Gram-Schmidt and Principal Components techniques, respectively. While, an overall accuracy and kappa coefficient of about 98.21% and 0.972 are obtained for the original Landsat OLI image. Overall, the results indicated slightly improvement in the accuracy of the maps produced using the specified Pan Sharpening algorithms compared to original Landsat image, which is significant where the accuracy of land cover map is very influential, such as military, precision agriculture, etc., applications in which land cover maps are used as the primary source.

Eventually, the study indicated that all the applied Pan Sharpening algorithms are appropriate in improving the accuracy of land cover mapping compared to original Landsat image, except Brovey technique. In this respect, the study confirmed the previous finding on which Brovey technique is not useful if preserving the radiometry of original scene is significant, nevertheless it is appropriate for producing visually appealing images (Nikolakopoulos, 2008). The findings of this study will be beneficial for the applications in which land cover maps are the primary sources, such as the impacts of global warming on the shrinkage of the lake in study area and ensuring food security of the region on urban sprawl.

Conclusions

In this study, the impact of Pan Sharpening was evaluated in improvement of image classification in Landsat 8 OLI imagery. In this respect, the Brovey, Gram-Schmidt, NNDiffuse, and Principal Components Pan Sharpening algorithms were applied to merge the Landsat OLI panchromatic band (15 m) with the Landsat OLI multispectral bands (30 m), to generate a new multispectral image with a higher spatial resolution (15 m). Image classification was implemented using support vector machine technique to classify the original Landsat and resulting fused images to four land cover types available in the study region including urban and built-up area, vegetation cover, bare land, and water body. Common training data was used for implementing image classification and accuracy assessment. The study revealed that comparable results are

obtained using the Gram-Schmidt, NNDiffuse, and Principal Components Pan Sharpening algorithms. However, NNDiffuse provided a superior result in Pan Sharpening and improvement of classification accuracy, with an overall accuracy and kappa coefficient of about 98.66% and 0.98, respectively. The study indicated suitability of the applied Pan Sharpening algorithms to enhance the accuracy of land-cover mapping compared to original Landsat image, except for Brovey technique which is suitable for producing visually appealing images. The findings of this study will be beneficial for the applications in which land cover maps are the primary sources, such as global warming, site selection and food security.

References

- Amarsaikhan, D., Saandar, M., Ganzorig, M., Blotevogel, H. H., Egshighlen, E., Gantuyal, R., Nergui, B., & Enkhjargal, D. (2012). Comparison of multisource image fusion methods and land cover classification. *International Journal of Remote Sensing*, 33, 2532–2550. <https://doi.org/10.1080/01431161.2011.616552>
- Aschbacher, J., & Lichtenegger, J. (1990). Complementary nature of SAR and optical data: A case study in the tropics. *Earth Observation Quarterly*, 31, 4–8.
- Bloom, A. L., Fielding, E. J., & Xiu-Yen, F. (1988). A demonstration of stereo photogrammetry with combined SIR-B and Landsat TM images. *International Journal of Remote Sensing*, 9, 1023–1038. <https://doi.org/10.1080/01431168808954911>
- Carper, W. J., Lillesand, T. M., & Kiefer, R. W. (1990). The use of intensity-hue saturation transformations for merging SPOT panchromatic and multispectral image data. *Photogrammetric Engineering & Remote Sensing*, 56, 459–467.
- Chavez, P. S., Sides, S. C., & Anderson, J. A. (1991). Comparison of three different methods to merge multiresolution and multispectral data- Landsat TM and SPOT panchromatic. *Photogrammetric Engineering & Remote Sensing*, 57, 295–303.
- De Béthune, S., Muller, F., & Donnay, J. P. (1998). Fusion of multispectral and panchromatic images by local mean and variance matching filtering techniques. In *Fusion of Earth Data* (pp. 28–30), Sophia, Antipolis, France.
- Dong, R., Fang, W., Fu, H., Gan, L., Wang, J., & Gong, P. (2021). High-resolution land cover mapping through learning with noise correction. *IEEE Transactions on Geoscience and Remote Sensing*, 60, 1–13. <https://doi.org/10.1109/TGRS.2021.3068280>
- Du, P., Liu, S., Xia, J., & Zhao, Y. (2013). Information fusion techniques for change detection from multi-temporal remote sensing images. *Information Fusion*, 14, 19–27. <https://doi.org/10.1016/j.inffus.2012.05.003>
- Eskandari, M., Homaei, M., Mahmoodi, S., Pazira, E., & Van Genuchten, M. T. (2015). Optimizing landfill site selection by using land classification maps. *Environmental Science and Pollution Research*, 22(10), 7754–7765. <https://doi.org/10.1007/s11356-015-4182-7>
- Ghayour, L., Neshat, A., Paryani, S., Shahabi, H., Shirzadi, A., Chen, W., Al-Ansari, N., Geertsema, M., Pourmehdi Amiri, M., Gholamnia, M., Dou, J., & Ahmad, A. (2021). Performance evaluation of Sentinel-2 and Landsat 8 OLI data for land cover/use classification using a comparison between machine learning algorithms. *Remote Sensing*, 13(7), 1349. <https://doi.org/10.3390/rs13071349>

- Ghorbanian, A., Kakooei, M., Amani, M., Mahdavi, S., Mohamadzadeh, A., & Hasanlou, M. (2020). Improved land cover map of Iran using Sentinel imagery within Google Earth Engine and a novel automatic workflow for land cover classification using migrated training samples. *ISPRS Journal of Photogrammetry and Remote Sensing*, 167, 276–288. <https://doi.org/10.1016/j.isprsjprs.2020.07.013>
- Gillespie, A. R., Kahle, A. B., & Walker, R. E. (1987). Color enhancement of highly correlated images. II. Channel ratio and “chromaticity” transformation techniques. *Remote Sensing of Environment*, 22, 343–365. [https://doi.org/10.1016/0034-4257\(87\)90088-5](https://doi.org/10.1016/0034-4257(87)90088-5)
- Hall, D., & Llinas, J. (2001). *Handbook of multisensor data fusion*. CRC Press. <https://doi.org/10.1201/9781420038545>
- Helmy, A. K., Nasr, A. H., & El-Taweel, G. S. (2010). Assessment and evaluation of different data fusion techniques. *International Journal of Computers*, 4, 107–115.
- Inglada, J., Vincent, A., Arias, M., Tardy, B., Morin, D., & Rodes, I. (2017). Operational high resolution land cover map production at the country scale using satellite image time series. *Remote Sensing*, 9(1), 95. <https://doi.org/10.3390/rs9010095>
- Karathanassi, V., Kolokousis, P., & Ioannidou, S. (2007). A comparison study on fusion methods using evaluation indicators. *International Journal of Remote Sensing*, 28, 2309–2341. <https://doi.org/10.1080/01431160600606890>
- Klonus, S., & Ehlers, M. (2007). Image fusion using the Ehlers spectral characteristics preservation algorithm. *GIScience & Remote Sensing*, 44, 93–116. <https://doi.org/10.2747/1548-1603.44.2.93>
- Klonus, S., & Ehlers, M. (2009). Performance of evaluation methods in image fusion. In *12th International Conference on Information Fusion Seattle* (pp. 1409–1416), WA, USA.
- Laben, C. A., Bernard, V., & Brower, W. (2000). *Process for enhancing the spatial resolution of multispectral imagery using pan-sharpening* (U.S. Patent No. 6,011,875). Eastman Kodak Company. <https://patents.google.com/patent/US6011875A/en>
- Lawrence, P. J., & Chase, T. N. (2010). Investigating the climate impacts of global land cover change in the community climate system model. *International Journal of Climatology*, 30(13), 2066–2087. <https://doi.org/10.1002/joc.2061>
- Leckie, D. (1990). Synergism of synthetic aperture radar and visible/infrared data for forest type discrimination. *Photogrammetric Engineering & Remote Sensing*, 56, 1237–1246.
- Li, Z., Bagan, H., & Yamagata, Y. (2018). Analysis of spatiotemporal land cover changes in Inner Mongolia using self-organizing map neural network and grid cells method. *Science of the Total Environment*, 636, 1180–1191. <https://doi.org/10.1016/j.scitotenv.2018.04.361>
- Liu, J. (2000). Smoothing filter-based intensity modulation: A spectral preserve image fusion technique for improving spatial details. *International Journal of Remote Sensing*, 21, 3461–3472. <https://doi.org/10.1080/014311600750037499>
- Meneses, B. M., Pereira, S., & Reis, E. (2019). Effects of different land use and land cover data on the landslide susceptibility zonation of road networks. *Natural Hazards and Earth System Sciences*, 19(3), 471–487. <https://doi.org/10.5194/nhess-19-471-2019>
- Meng, X., Dodson, A., Jixian, Z., Yanhui, C., Chun, L., & Geary, K. (2011). Geospatial data fusion for precision agriculture. In *International Symposium on Image and Data Fusion (ISIDF)* (pp. 1–4), Tengchong, China. <https://doi.org/10.1109/ISIDF.2011.6024218>
- Nikolakopoulos, K. G. (2008). Comparison of nine fusion techniques for very high resolution data. *Photogrammetric Engineering & Remote Sensing*, 74, 647–659. <https://doi.org/10.14358/PERS.74.5.647>
- Oetter, D. R., Cohen, W. B., Berterretche, M., Maiersperger, T. K., & Kennedy, R. E. (2001). Land cover mapping in an agricultural setting using multiseasonal Thematic Mapper data. *Remote Sensing of Environment*, 76(2), 139–155. [https://doi.org/10.1016/S0034-4257\(00\)00202-9](https://doi.org/10.1016/S0034-4257(00)00202-9)
- Pal, M., & Foody, G. M. (2012). Evaluation of SVM, RVM and SMLR for accurate image classification with limited ground data. *IEEE Journal of Selected Topics in Applied Earth Observations and Remote Sensing*, 5, 1344–1355. <https://doi.org/10.1109/JSTARS.2012.2215310>
- Pérez-Hoyos, A., Rembold, F., Kerdiles, H., & Gallego, J. (2017). Comparison of global land cover datasets for cropland monitoring. *Remote Sensing*, 9(11), 1118. <https://doi.org/10.3390/rs9111118>
- Petropoulos, G. P., Kontoes, C. C., & Keramitsoglou, I. (2012). Land cover mapping with emphasis to burnt area delineation using co-orbital ALI and Landsat TM imagery. *International Journal of Applied Earth Observation and Geoinformation*, 18, 344–355. <https://doi.org/10.1016/j.jag.2012.02.004>
- Pflugmacher, D., Rabe, A., Peters, M., & Hostert, P. (2019). Mapping pan-European land cover using Landsat spectral-temporal metrics and the European LUCAS survey. *Remote Sensing of Environment*, 221, 583–595. <https://doi.org/10.1016/j.rse.2018.12.001>
- Pohl, C., & Van Genderen, J. (1998). Review article Multisensor image fusion in remote sensing: Concepts, methods and applications. *International Journal of Remote Sensing*, 19, 823–854. <https://doi.org/10.1080/014311698215748>
- Qiu, X., & Qiu, X. (2011). Wetland monitor for Poyang Lake Ecological Economic Region based on Landsat-7 sensing data. In *2nd International Conference on Artificial Intelligence, Management Science and Electronic Commerce (AIMSEC)* (pp. 6495–6498), Deng Feng, China.
- Rokni, K., Marghany, M., Hashim, M., & Hazini, S. (2011). Comparative statistical-based and color-related pan sharpening algorithms for ASTER and RADARSAT SAR satellite data. In *2011 IEEE International Conference on Computer Applications and Industrial Electronics (ICCAIE)* (pp. 618–622), Penang, Malaysia. <https://doi.org/10.1109/ICCAIE.2011.6162208>
- Santos, C., & Messina, J. P. (2008). Multi-sensor data fusion for modeling African palm in the Ecuadorian Amazon. *Photogrammetric Engineering & Remote Sensing*, 74, 711–723. <https://doi.org/10.14358/PERS.74.6.711>
- Schowengerdt, R. A. (1980). Reconstruction of multispatial, multispectral image data using spatial frequency content. *Photogrammetric Engineering & Remote Sensing*, 46, 1325–1334.
- Shakya, A. K., Ramola, A., & Vidyarthi, A. (2021). Exploration of pixel-based and object-based change detection techniques by analyzing ALOS PALSAR and LANDSAT Data. In N. Gupta, P. Chatterjee, & T. Choudhury (Eds.), *Smart and sustainable intelligent systems* (pp. 229–244). Scrivener Publishing. <https://doi.org/10.1002/9781119752134.ch17>
- Solberg, A. H. S., Jain, A. K., & Taxt, T. (1994). Multisource classification of remotely sensed data: Fusion of Landsat TM and SAR images. *IEEE Transactions on Geoscience and Remote Sensing*, 32, 768–778. <https://doi.org/10.1109/36.298006>
- Sood, V., Gusain, H. S., Gupta, S., Taloor, A. K., & Singh, S. (2021). Detection of snow/ice cover changes using subpixel-based change detection approach over Chhota-Shigri glacier,

- Western Himalaya, India. *Quaternary International*, 575, 204–212. <https://doi.org/10.1016/j.quaint.2020.05.016>
- Suits, G., Malila, W., & Weller, T. (1988). Procedures for using signals from one sensor as substitutes for signals of another. *Remote Sensing of Environment*, 25, 395–408. [https://doi.org/10.1016/0034-4257\(88\)90111-3](https://doi.org/10.1016/0034-4257(88)90111-3)
- Sun, W., Chen, B., & Messinger, D. (2014). Nearest neighbor diffusion-based pan-sharpening algorithm for spectral images. *Optical Engineering*, 53(1), 013107. <https://doi.org/10.1117/1.OE.53.1.013107>
- Vijayalakshmi, S., Kumar, M., & Arun, M. (2021). A study of various classification techniques used for very high-resolution remote sensing [VHRRS] images. *Materials Today: Proceedings*, 37, 2947–2951. <https://doi.org/10.1016/j.matpr.2020.08.703>
- Walker, J. J., De Beurs, K. M., Wynne, R. H., & Gao, F. (2012). Evaluation of Landsat and MODIS data fusion products for analysis of dryland forest phenology. *Remote Sensing of Environment*, 117, 381–393. <https://doi.org/10.1016/j.rse.2011.10.014>
- Yocky, D. A. (1995). Image merging and data fusion by means of the discrete two dimensional wavelet transform. *Journal of the Optical Society of America*, 12, 1834–1841. <https://doi.org/10.1364/JOSAA.12.001834>
- Zhang, Y. (2002). Automatic image fusion: A new sharpening technique for IKONOS multispectral images. *GIM International*, 16, 54–57.
- Zhang, Y. (2004). Understanding image fusion. *Photogrammetric Engineering & Remote Sensing*, 70, 657–661. <https://doi.org/10.14358/PERS.70.7.821>
- Zhu, R. (2011). Fusion of airborne SAR image and color aerial image for land use classification. In *MIPPR 2011: Remote Sensing Image Processing, Geographic Information Systems, and Other Applications* (Vol. 8006). <https://doi.org/10.1117/12.898744>
- Zope, P. E., Eldho, T. I., & Jothiprakash, V. (2017). Hydrological impacts of land use–land cover change and detention basins on urban flood hazard: A case study of Poisar River basin, Mumbai, India. *Natural Hazards*, 87(3), 1267–1283. <https://doi.org/10.1007/s11069-017-2816-4>